Tunable Multifunctional Mesoporous Silica Microdots Arrays by Combination of Inkjet Printing, EISA, and Click Chemistry

ARTICLE *in* CHEMISTRY OF MATERIALS · NOVEMBER 2012

Impact Factor: 8.35 · DOI: 10.1021/cm3022769

13 AUTHORS, INCLUDING:

Olivia De Los Cobos
University of Limoges
12 PUBLICATIONS **27** CITATIONS
SEE PROFILE

Cedric Boissiere
Pierre and Marie Curie University - Paris 6
220 PUBLICATIONS **5,390** CITATIONS
SEE PROFILE

Michel Wong Chi Man
French National Centre for Scientific Research
194 PUBLICATIONS **3,610** CITATIONS
SEE PROFILE

CHEMISTRY OF MATERIALS

Article

pubs.acs.org/cm

Tunable Multifunctional Mesoporous Silica Microdots Arrays by Combination of Inkjet Printing, EISA, and Click Chemistry

Olivia De Los Cobos,*[,†] Bruno Fousseret,[†] Martine Lejeune,*[,†] Fabrice Rossignol,[†] Maggy Dutreilh-Colas,[†] Claire Carrion,[‡] Cédric Boissière,[§] François Ribot,[§] Clément Sanchez,[§] Xavier Cattoën,*[,⊥] Michel Wong Chi Man,[⊥] and Jean-Olivier Durand[⊥]

[†]Laboratoire de Science des Procédés Céramiques et de Traitements de Surface (SPCTS), UMR CNRS 7315, CEC, 12 rue Atlantis, 87068 Limoges, France

[‡]Plateforme Cytométrie-Imagerie-Mathématiques, UMR CNRS 6101, Faculté de médecine, 2 rue du Dr Marcland, 87025 Limoges Cedex, France

[§]Laboratoire de Chimie de la Matière Condensée de Paris, UMR CNRS 7574, Université Pierre et Marie Curie Paris VI, Collège de France, 11 place Marcelin Berthelot, 75005 Paris, France

[⊥]Institut Charles Gerhardt Montpellier (UMR 5253 CNRS-UM2-ENSCM-UM1), place Eugène Bataillon, 34095 Montpellier, France

ABSTRACT: A novel technique combining inkjet printing (IJP), evaporation-induced self-assembly (EISA), and click chemistry is implemented for elaborating mesoporous silica-based multifunctional microdots arrays. The microdots are in situ azide-functionalized with (3-azidopropyl)triethoxysilane (AzPTES). AzPTES is directly added to the initial sol before IJP and co-condenses with the silica precursor (TEOS) during the evaporation-induced self-assembly (EISA) of micelles on the substrate. After extracting the surfactants to release the porosity, model alkynes, namely propargyl alcohol, methyl pent-4-ynoate, ethynylferrocene, and *N*-propargyl-4-amino-1,8-naphthalimide, are grafted by the azide−alkyne CuAAC click reaction. The demonstration is established that the click reaction is nearly quantitative and occurs in the whole volume of the microdots attesting the accessibility of the azide groups. By integrating an alkyne-containing silylated precursor in a similar route, azide-containing functional groups are anchored in the microdots by click reaction. A demonstration of the multifunctionalization of such microdots arrays is achieved by reacting clickable dyes on alternate alkyne- and azide-functionalized lines of microdots, as evidenced by confocal fluorescence microscopy. Such multifunctional mesoporous silica microdots arrays offer promising perspectives for biosensing applications.

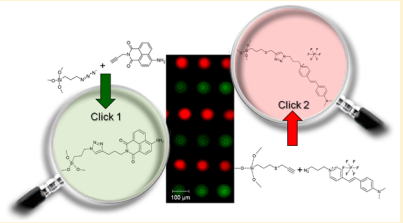

KEYWORDS: *mesoporous silica, inkjet printing, click chemistry, fluorescent probes*

INTRODUCTION

The inkjet printing (IJP) technology offers promising opportunities in the field of sensors fabrication thanks to its flexibility, current resolution, and capability to build in patterned arrays of microdots that can be specifically and individually functionalized for sensing by using a multiheads printing device. Thus, IJP has already been used to produce glucose,[1] antibodies sensors,[2] and DNA arrays.[3,4] However, in these previous studies, the functionalization has been achieved by introducing biomolecules directly inside the ink before printing. As a result, the biomolecules may be damaged during the ejection.[5] In contrast, in the present work, clickable mesoporous silica microdots arrays are deposited by a one-pot IJP process, allowing a safe and selective postfunctionalization by copper-catalyzed azide−alkyne cyloaddition (CuAAC) click reactions.

Click chemistry is a well-known and powerful tool to covalently bind (bio)molecules bearing terminal alkynes onto azide-functionalized surfaces.[6−10] Such a regioselective and orthogonal copper-catalyzed reaction between azides and alkynes has been successfully applied to mesoporous silica with high yields.[11−13] The increasing availability of clickable biomolecules, namely oligonucleotides[14] or proteins,[15] suitable for anchoring into the "ready to click" mesoporous silica microdots arrays justifies the use of click chemistry for the selective functionalization in prospects of multianalyte biosensing applications.

In addition to its remarkable ability to be functionalized by organic functions through soft chemistry processes,[16] mesoporous silica is an interesting material for sensing applications thanks to its ordered structure[17] and its high specific surface area that can exceed 1000 $m^2\ g^{-1}$, which could provide a great asset in terms of sensitivity because of the potential density of immobilized target biomolecules is relevant for the detection stage while the device can be miniaturized. Besides its chemical inertia and its mechanical strength in biological environment,[17] subjoined arguments for its integration in robust biosensors are expected. In addition, a biosensor transducer can benefit from

Received: July 19, 2012
Revised: October 24, 2012
Published: October 26, 2012

dx.doi.org/10.1021/cm3022769 | *Chem. Mater.* 2012, 24, 4337−4342

its optical properties, such as transparency and reflectivity that are particularly adapted for fluorescence detection techniques.[18]

The inkjet printing is a patterning process of choice for materials such as ceramics[19,20] and namely for mesoporous silica as demonstrated by Mougenot et al.[21] Indeed, the computer-controlled deposition, associated with 50 μm-aperture nozzles of the printing head, enables to achieve 100 μm microdots networks that can be organized on demand in prospects of a miniaturized array sensor device.

Moreover, microdots can be specifically and individually functionalized for sensing by using a multiheads printing device. In fact, by developing multiple inks, which will be thereafter injected in the multiheads apparatus, an intercrossed network can be produced where each microdot has a specific task to perform. The variety of inks, combined with the large library of clickable biomolecules, is expected to offer a multiplexing device.

Its noncontact character, the weak amount of raw material required, the reduced rate of waste, and the direct mask-free fabrication lead to a relatively low-cost process, which is relevant for mass production of microarrays in the near future.

Herein, we demonstrate the potential of combining mesoporous silica microdot arrays obtained by IJP/EISA together with click chemistry to easily fabricate innovative multifunctional arrays.

EXPERIMENTAL SECTION

The silica source (TEOS), propargyl alcohol, ethynylferrocene, and the nonionic structuring agent (Pluronic F127) were purchased from Sigma-Aldrich. The hydrophobic additive (TFTS) was purchased from ABCR. The substrates consist in hydrophilic silicon wafers with hydroxylated native silicon oxide (Si-Mat, ref SW 150 mm/p/boron). The following compounds (3-azidopropyl)triethoxysilane (**AzPTES**),[11] (3-(prop-2-yn-1-yl)thiopropyl)triethoxysilane **1**,[13] methyl pent-4-ynoate **3**,[11] and the clickable dyes **5** and **6**[22] were prepared according to published procedures. The propargylmelamine and the dye-labeled thymine were synthesized according to the following procedures.

Propargylmelamine 7. 2-Chloro-4,6-diamino-1,3,5-triazine (1.0 g, 6.9 mmol) was added to a mixture of propargylamine (0.45 g, 8.2 mmol) and $NaHCO_3$ (0.57 g, 6.9 mmol) in EtOH/H_2O (120 mL, 1:1).[23] The reaction mixture was heated at 80 °C; after 3−4 h, a clear solution was obtained. The solution was heated for a further 20 h and filtered. The filtrate was evaporated and dried under vacuum. Propargylmelamine was isolated as a white powder and used in the following step without further purification. Yield 1.0 g, 88%.

^{1}H NMR (DMSO-d_6, 400 MHz): δ 6.83 (t, J = 6.1 Hz, 1H); 6.0—6.3 (br, 4H); 3.96 (dd, J = 6.1 and 2.5 Hz, 2H); 3.00 (t, J = 2.5 Hz, 1H). ^{13}C NMR (DMSO-d_6, 100 MHz): δ 167.0; 166.0; 82.6; 72.2; 29.1. HRMS (ESI+): calcd for $C_6H_9N_6$,165.0889; found, 165.0877.

Dye-Labeled Thymine 8. Under an argon atmosphere, 1-propargylthymine (0.16 g, 1.0 mmol) and **6** (0.45 g, 1.0 mmol) were dissolved in a 1:1 mixture of acetonitrile and water (4 mL). $CuBr(PPh_3)_3$ (46 mg, 0.05 mmol) was added, and the mixture was then stirred at room temperature until disappearance of the starting reagents (ca. 30 h). The mixture was concentrated then the crude product was purified by silica gel chromatography ($CHCl_3$/MeOH 5:1). Yield: 375 mg, 79%.

^{1}H NMR (DMSO-d_6, 400 MHz): δ = 11.31 (s, 1H); 8.71 (d, J = 6.7 Hz, 2H); 8.08 (s, 1H); 8.04 (d, J = 7.3 Hz, 2H); 7.95 (d, J = 16.1 Hz, 1H); 7.60 (m, 3H); 7.16 (d, J = 16.1 Hz, 1H); 6.80 (d, J = 9.1 Hz, 2H); 4.88 (s, 2H); 4.45 (m, 4H); 3.02 (s, 6H); 2.49 (m, 2H); 1.74 (s, 3H). ^{13}C NMR (DMSO-d_6, 100 MHz): δ = 164.2; 153.9; 152.0; 150.7; 143.6; 142.3; 141.1; 140.9; 130.2; 123.7; 122.4; 122.3; 117.0; 111.9; 108.8; 56.7; 46.4; 42.2; 39.7; 30.5; 11.9. HRMS (ESI+): calcd for $C_{26}H_{30}N_7O_2$: 472.2461; found: 472.2458.

On the basis of a previous work,[24] an azide-based ink formulation containing (3-azidopropyl)triethoxysilane (AzPTES, Chart 1) was

Chart 1. Compounds Used in This Study

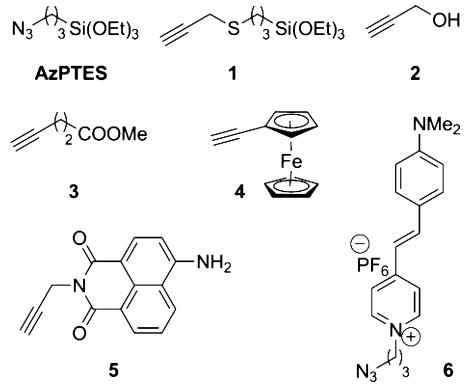

tested, with the following molar composition: 1:0.05:0.10:0.006:5:0.02:20 TEOS:TFTS:AzPTES:F127:H_2O:HNO_3:EtOH. The presence of tridecafluorooctyltriethoxysilane (TFTS) as hydrophobic surfactant is necessary in order to guarantee the reliability of the ejection because of the hydrophilic nature of the printing-head. The sol was prepared by mixing TEOS (7.74 g, 37.2 mmol), TFTS (0.95 g, 1.9 mmol), AzPTES (0.92 g, 3.7 mmol), and ethanol (33.4 mL). Afterward, the triblock copolymer Pluronic F127 (M = 12 500 Da, 2.81 g, 0.2 mmol) was incorporated and the as-obtained solution was mixed by magnetic stirring at 30 °C until complete dissolution of F127. The solution was then cooled down to room temperature before adding the nitric acid−water mixture (H_2O/HNO_3 0.235 mol L^{-1}, 3.34 mL, 0.78 mmol (HNO_3), and 186 mmol (H_2O)). Finally, the solution was placed under rotative agitation for 48 h. The as-synthesized solution (i.e., ink) exhibits a surface tension of 22.8 mN/m and an apparent viscosity of 5 mPa.s. The corresponding ratio of ejection ratio, $Re/We^{1/2}$, is equal to 4.6, i.e., in the adequate range (1−10) for an appropriate ejection.

A similar procedure was employed, replacing AzPTES by **1** (1.13 g, 3.7 mmol). The as-synthesized solution (i.e., ink) exhibits a surface tension of 22.9 mN/m and an apparent viscosity of 4.2 mPa.s. The corresponding ejection ratio, $Re/We^{1/2}$, is equal to 5.3, i.e., in the adequate range (1−10) thus allowing the ejection.

The IJP equipment used is a commercial drop-on-demand one with piezoelectric printing heads (Ceraprinter L01163-Ceradrop, Ester Technopole, BP 36921, Limoges, France). The printing head displacement has a resolution of 0.5 μm, a reproducibility of 2 μm, and an accuracy of 2 μm. The current resolution achieved is between 30 and 50 μm. Additional technical data are given in the patent PCT/RF04/02150. Before the fabrication of the microdots arrays, the electric pulse applied to the nozzle was adjusted to get a consistent droplet ejection. This adjustment was carried out by capturing stroboscopically backlit images of the ejection with a CCD video camera. Five layers microdots arrays were deposited under controlled conditions of temperature (293K) and humidity (50%), by 10 min delayed successive deposits of droplets on a same location[24] onto hydrophilic silicon wafers with hydroxylated native silicon oxide.

The obtained patterns (Figure 1) consisted of well-resolved microdots arrays (diameter of 96 μm spaced out of 40 μm, height of 1.5 μm) illustrating the capability of inkjet printing to allow fabricating highly resolved and complex patterns. The as-obtained microdots arrays were then submitted to a mild thermal treatment (130 °C, 48 h) in order to stiffen the inorganic network without damaging the functional organic groups. However, the temperature of that thermal treatment is not high enough to burn out the structuring agent (F127). Therefore, a subsequent Soxhlet chemical extraction in acidified ethanol (10 vol %) was performed during 24 h to remove the F127 structuring agent from the porosity,[25] so that all the pores became available for the "click" postfunctionalization (Scheme 1).

dx.doi.org/10.1021/cm3022769 | Chem. Mater. 2012, 24, 4337−4342

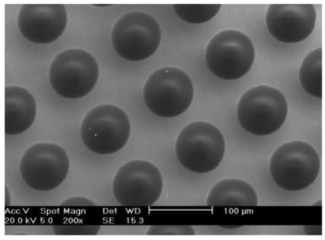

Figure 1. SEM image of azide-functionalized mesoporous silica 5-layers microdots array deposited onto a silicon wafer.

Scheme 1. Click Functionalization: (1) Surfactant Removal, (2) CuAAC Reaction

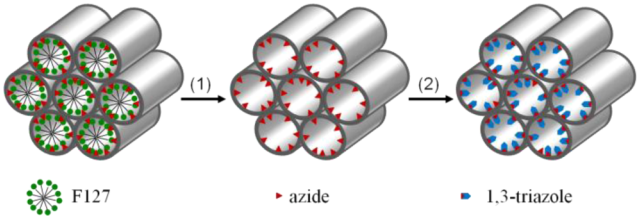

The click reaction was performed as follows, based on previous studies.[11] Azide- or alkyne-functionalized Soxhlet-washed microdots arrays (ca. 1 cm^2, theoretical functionalization degree 5.6×10^{-5} mmol cm^{-2}) were immersed in a solution of the corresponding alkyne or azide (1.7×10^{-3} mmol) in a water/t-BuOH 1:1 mixture (20 mL) containing $CuSO_4.5H_2O$ (14 mg, 5.6×10^{-2} mmol) and sodium ascorbate (22 mg, 0.11 mmol) for 24 h. After 12 h, another portion of sodium ascorbate (22 mg, 0.11 mmol) was added. Once the click reaction had proceeded, alternate washings of the wafer with sodium *N,N*-diethyldithiocarbamate in methanol (0,1 M, 5 mL) and pure methanol (5 mL) were performed to remove the residual copper salts. These washing steps were repeated three times before submitting the clicked microdots to a final Soxhlet extraction in ethanol for 24 h, in order to fully remove all physisorbed molecules from the porosity.

2D small-angle X-ray scattering (2D-SAXS) were performed using a Rigaku S-max 3000 diffractometer. Scanning electron microscopy (SEM) images were obtained with a Philips XL30 at 20 kV. Transmission electron microscopy (TEM) images were obtained with a Jeol 2100 F apparatus at 200 kV. Micro-Raman spectra have been recorded on a T64000 spectrophotometer (HORIBA Jobin Yvon) in the backscattering mode at 514 nm. Raman mapping have been obtained using an In Via Reflex spectrophotometer (Renishaw) in the Streamline mode illumination at 532 nm. Confocal laser scanning microscopy (CLSM) images were obtained with a Zeiss LSM 510 META Instruments using excitation wavelengths of 405 and 543 nm for the 4-amino-1,8-naphtalimide dye **5** and the red dye **6**, respectively. Fourier transform infrared spectroscopy (FT-IR) spectra were obtained in a transmission mode using a Perkin-Elmer Spectrum One spectrometer.

RESULTS AND DISCUSSION

The main issues of this study were to evaluate the influence of the incorporation of azide in the mesoporous silica structure elaborated by one-pot IJP process and to demonstrate that a postfunctionalization by click chemistry is efficient and selective within the microdots network.

1. Effect of the incorporation of Azide on the Mesoporous Structure. 2D-SAXS measurements of the deposited microdots arrays (Figure 2a) revealed a diffuse diffraction ring, characteristic of a wormlike structure of the mesoporosity,[26] which was confirmed by TEM observations (Figure 2b). Previous studies had already shown that such inkjet printed microdots arrays made without AzPTES

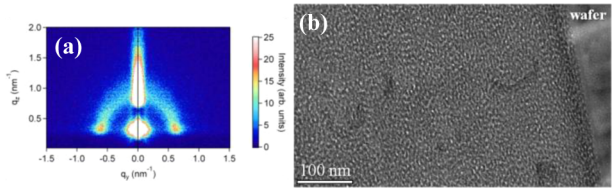

Figure 2. Structural organization of five-layer microdots made with a 10 mol % AzPTES solution aged for 48 h: (a) 2D SAXS pattern and (b) TEM image of a microdot cross-section.

exhibited a centered rectangular structure.[23] The loss of regular mesostructure organization upon the addition of AzPTES could result from the large amount of organosilane (i.e., 15 mol % overall). In fact, as observed by Matheron,[27] a saturation of silica oligomers is observed as the organosilane content increases, which limits the percolation phenomenon around the surfactant and consequently the mesostructure organization. Nevertheless, considering the fact that the microdots usually exhibit an open porosity,[24] a disordered wormlike structure might be sufficient to achieve a significant sensitivity for the targeted application.

2. CuAAC Functionalization of the Mesoporous Silica and Validation of the Click Reaction within the Microdots. The presence of the azide moieties before and after the template extraction was ascertained by the azide band at 2100 cm^{-1} in FTIR (Figure 3B,C), whereas this band does not appear in mesoporous silica without the introduction of AzPTES(Figure 3A).

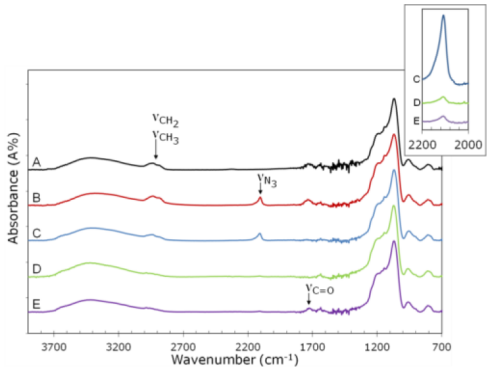

Figure 3. FT-IR analyses of mesoporous silica microdots: (A) unfunctionalized, (B) azide-functionalized before F127 extraction, (C) azide-functionalized after F127 extraction, (D) after "click" reaction with alkyne **2**, and (E) after "click" reaction with alkyne **3** and in the top right corner, the magnification of the azide band.

To evaluate the potentiality of these microdots arrays toward the CuAAC postfunctionalization reaction, four alkynes, namely propargyl alcohol **2**, methyl pent-4-ynoate[11] **3**, ethynylferrocene **4**, and *N*-propargyl-4-amino-1,8-naphthal-imide[22] **5** (Chart 1), were reacted under standard conditions [alkyne, $CuSO_4$/sodium ascorbate catalytic system, water/t-BuOH (1:1) solvent mixture for 24 h]. After the click reaction had proceeded, successive washings with sodium *N,N*-diethyldithiocarbamate in methanol and pure methanol were performed to remove the residual copper salts and alkynes remaining in the porosity. The success of the click reaction was evidenced after the reaction with propargyl alcohol **1** by the almost complete disappearance of the azide band (Figure 3D).[11] The remaining azide peak likely corresponds to groups trapped in the silica walls and thus

dx.doi.org/10.1021/cm3022769 | *Chem. Mater.* 2012, 24, 4337−4342

not accessible, an approximate anchoring of 93% being estimated from this spectrum considering that spectrum C represents the total amount of azide.

The functionalization of the mesoporous silica was also confirmed by the reaction with methyl pent-4-ynoate **3** (Figure 3E). This molecule exhibits a specific ester vibration band at 1730 cm^{-1} in IR.[28] As expected, both the decrease of the azide vibration intensity and the appearance of the ester characteristic band at 1730 cm^{-1} were observed even after vigorous washing. Furthermore, an approximate anchoring of 93% was also estimated in this case.

3. Click Reaction with Ethynylferrocene Monitoring by Raman Spectroscopy. A click reaction between azide-functionalized microdots arrays and ethynylferrocene **4** was performed in order to graft an electroactive molecule within the mesoporous silica microdots, thus demonstrating the potential application as electrochemical sensor. Ethynylferrocene was reacted under the above-mentioned conditions. The drastic increase of the vibration intensity band at 1600 cm^{-1} after the click reaction with ethynylferrocene (Figure 4B) was attributed

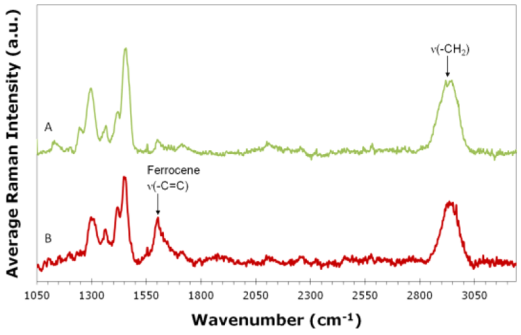

Figure 4. Raman spectra of (A) azide-functionalized after F127 extraction, and (B) after click reaction with ethynylferrocene.

to characteristic ferrocene band with ν(C=C) aromatic vibrations.[29] It can be noted that $\nu(CH_2)$ bending vibration mode presents a high intensity at 2800−3000 cm^{-1}, even after the washing step to remove the F127 surfactant, because of the CH_2 groups in AzPTES and TFTS incorporated in the mesoporous silica.

Following the determination of the characteristic ferrocene band, a Raman mapping of the microdots array was performed in order to visualize the ferrocene spatial distribution. The image is reconstructed from the integrated intensity of the ferrocene band (between 1580 and 1620 cm^{-1}) obtained from 13158 spectra. The colors contrast represent the variation of the intensity fluctuation associated with the ν(C=C) aromatic vibrations.

First, a Raman mapping on a 110 × 550 μm^2 surface covered by a four microdots raw, with a 1 μm spatial resolution, allowed us to evidence the well distribution of the ferrocene over the whole surface of the dots (Figure 5a,b).

Then, a second mapping on one microdot with a submicrometer resolution (0.5 μm) helps us to get more detailed information (Figure 5c). Obviously the vibrationnal ferrocene signature exists all over the microdot. The intensity variation of colors that can be observed in Figure 5c, corresponding to a higher intensity on the microdot center and a lower intensity on the microdot edges, is only due to the curvature variation of the dots.

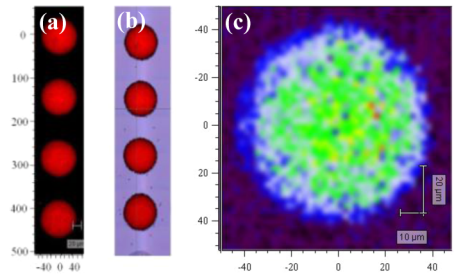

Figure 5. (a) Raman mapping of a click-functionalized microdot row showing the ethynylferrocene **4** spatial distribution, (b) superposition of the Raman mapping with optical micrograph of the microdots, and (c) Raman mapping of a single click-functionalized microdot evidence the ethynylferrocene **4** spatial distribution with a fine spatial resolution.

4. Selectivity of the Click Reaction Demonstrated by Fluorescent Probes. An array composed of intercrossed networks of azide-functionalized and unfunctionalized microdots was produced (Figure 6a). After removing the surfactant,

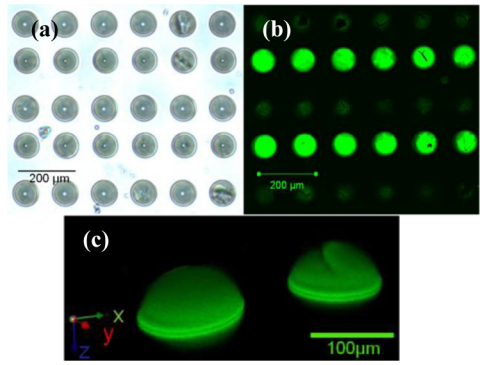

Figure 6. (a) Optical and (b) confocal fluorescence images of alternate rows after clicking with **5**. (c) 3D confocal microscopy reconstitution of two microdots.

immersing the wafer in a reaction mixture containing **5**, copper sulfate, and sodium ascorbate in a *t*-BuOH-H_2O mixture, then carefully washing the wafer, we demonstrated the selectivity of the click reaction using confocal microscopy. Indeed, the image obtained shows that the fluorescent groups of **5** are selectively localized on the azide-functionalized rows, whereas the unfunctionalized rows only exhibit a negligible residual fluorescence (Figure 6b). This observation underlines the fact that the alkyne functions were truly reacted with the azide moieties within the silica network and not just physically entrapped in the pores. Moreover, 3D fluorescence responses, evidenced by confocal laser scanning microscopy (Figure 6c), pointed out the occurrence of the functionalization throughout the volume of the 5-layers microdots. This result suggests that the overall functionalization of the microdots array can be amplified by increasing the volume of the microdots, which is easily achievable by stacking more layers with inkjet printing process. This demonstration with fluorophores highlights that the inkjet patterned surface is particularly adapted for scanning microscopy analysis of the resulting signal.

5. Multipatterning and Multifunctionalization Performance Highlighted by Fluorescence Microscopy. A complementary click route toward functional microdots was also investigated: an ink containing the alkyne-based organotriethoxysilane **1**[13] with the following composition:

dx.doi.org/10.1021/cm3022769 | *Chem. Mater.* 2012, 24, 4337−4342

1:0.05:0.10:0.006:5:0.02:20 TEOS:TFTS:**1**:F127:H_2O:HNO_3:EtOH was successfully ejected after an optimized aging time of 48 h. The resulting microdots array was functionalized with the red dye **6**.[22]

To demonstrate the specificity of the CuAAC reaction and its potential to obtain multifunctional arrays, we obtained a wafer printed with alternate rows of azide- and alkyne-functionalized microdots by the coupled EISA/IJP technique by using successively two different printing heads. After thermal treatment and surfactant removal, the object was submitted to two successive CuAAC reactions: the first one was carried out with the alkyne-functionalized green fluorophore **5**, whereas the second one was realized with the azide-containing red fluorophore **6**. The alkyne-based fluorophore **5** only reacted with the azide-functionalized rows (Figure 7a), whereas the

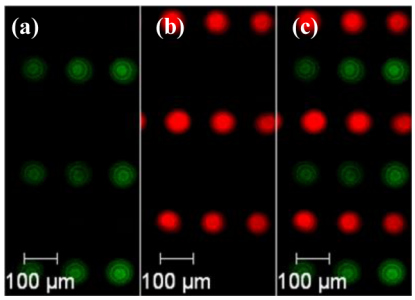

Figure 7. Confocal fluorescence images of bifunctional microdots alternate rows (a) reacted only with **5**, (b) reacted only with **6**, and (c) successively reacted with **5** and **6**.

alkyne-functionalized microdots specifically reacted with **6**, without any mixture (Figure 7c). To confirm these observations, we could also achieve the same bifunctionalization when reversing the two steps (Figure 7b). These results underline the specificity of the "click" reaction and highlight the possibility to specifically functionalize microdots in order to collect one type of fluorescent signal per row. This scheme can be extended to multifunctional microdots arrays. This combination offers to multiply the detection possibilities with a large library of target biomolecules by varying the inkjet-printed microdot nature and the click-reacted derivative probes.

6. Toward Biosensor Applications. DNA biosensors are based on the interactions between two oligonucleotides sequences, the molecular recognition occurring between two complementary nucleobases by hydrogen bonds. Thus, melamine with alkyne end-function was immobilized on the azide-functionalized rows of an alternate network containing also pure SiO_2 neutral rows, according to the standard click reaction. The as-obtained microdots array was immersed in chloroform with fluorescent labeled thymine, which exhibits a three hydrogen bond interaction with melamine.[30] After rinsing, the thymine remained on the melamine-functionalized row, as observed in Figure 8b, demonstrating that the interactions were sufficient to allow selection and detection by fluorescence microscopy on the microdots array.

■ CONCLUSIONS

This study demonstrates the interest of combining IJP, EISA, and CuAAC-click chemistry to get multifunctional micropatterned surfaces. In the whole process, the IJP technique brings more specifically its potential in terms of selectivity, resolution and flexibility. In particular, the capability to

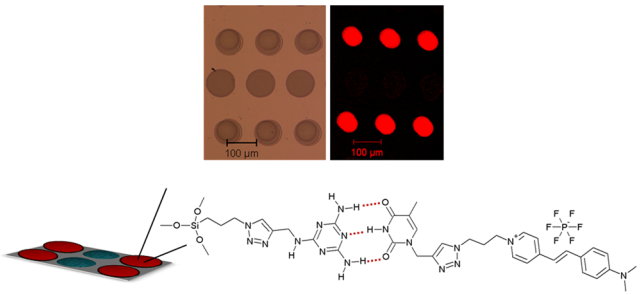

Figure 8. (a) Optical and (b) confocal fluorescence micrographs of the alternate rows after molecular recognition of fluorescent labeled thymine.

specifically functionalize each microdot in a one-pot process by using a multiheads printing device is very promising to click afterward a large range of molecules. The click reaction within the mesoporous silica microdots has been demonstrated and its interest in detection has been revealed especially with the use of *N*-propargyl-4-amino-1,8-naphthalimide and ethynylferrocene, which can be implied in fluorescence or electrochemical based detection. Therefore, these multiplexing arrays might be suitable for fluorescent revelation as well as redox targets.

■ AUTHOR INFORMATION

Corresponding Author

*E-mail: olivia.de-los-cobos@etu.unilim.fr (O.d.l.C.); xavier.cattoen@enscm.fr (X.C.); martine.lejeune@unilim.fr (M.L.).

Notes

The authors declare no competing financial interest.

■ ACKNOWLEDGMENTS

We are grateful to the CNRS, the French Higher Education and Research Ministry, and the Limousin Region for financial supports. We thank P. Carles for the SEM images, B. Soulestin for the TEM analyses, M. Selmane for the Gi-SAXS characterizations, Dr M. Granier, Prof. T. Merle-Méjean, and Dr. J. Cornette for the FT-IR studies, M. Belleil from RENISHAW company for the Raman mapping, Dr N. Moitra and K. Bürglová for the synthesis of some chemicals, and M. Chambon and Ceradrop company for inkjet printing technical support.

■ REFERENCES

(1) Yun, Y. H.; Lee, B. K.; Choi, J. S.; Kim, S.; Yoo, B.; Kim, Y. S.; Park, K.; Choy, Y. W. *Anal. Sci.* **2011**, *27*, 375.

(2) Hasenbank, M. S.; Edwards, T.; Fu, E.; Garzon, R.; Kosar, T. F.; Look, M.; Mashadi-Hossein, A.; Yager, P. *Anal. Chim. Acta* **2008**, *611*, 80.

(3) Cooley, P. W.; Hinson, D.; Trost, H. J.; Antohe, B.; Wallace, D. B. *Methods Mol. Biol.* **2001**, *170*, 117.

(4) Allain, L. R.; Stratis-Cullum, D. N.; Vo-Dinh, T. *Anal. Chim. Acta* **2004**, *518*, 77.

(5) Nishioka, G. M.; Markey, A. A.; Holloway, C. K. *J. Am. Chem. Soc.* **2004**, *126*, 16320.

(6) Rostovtsev, V. V.; Green, L. G.; Fokin, V. V.; Sharpless, K. B. *Angew. Chem., Int. Ed.* **2002**, *14*, 2596.

(7) Tornøe, C. W.; Meldal, M. *Proceedings of the 17th American Peptide Symposium*; Lebl, M., Houghten, R. A., Eds.; Kluwer Academic Publishers: Norwell, MA, 2001; p 263.

(8) Tornøe, C. W.; Christensen, C.; Meldal, M. *J. Org. Chem.* **2002**, *67*, 3057.

(9) Nandivada, H.; Jiang, X.; Lahann, J. *Adv. Mater.* **2007**, *19*, 2197.

(10) Binder, W. H.; Sachsenhofer, R. *Macromol. Rapid Commun.* **2008**, *29*, 952.
(11) Malvi, B.; Sarkar, B. R.; Pati, D.; Mathew, R.; Ajithkumarb, T. G.; Sen Gupta, S. *J. Mater. Chem.* **2009**, *19*, 1341.
(12) Nakazawa, J.; Stack, T. D. P. *J. Am. Chem. Soc.* **2008**, *130*, 14360.
(13) Moitra, N.; Trens, P.; Raehm, L.; Durand, J.-O.; Cattoën, X; Wong Chi Man, M. *J. Mater. Chem.* **2011**, *21*, 13476.
(14) El-Sagheerab, A. H.; Brown, T. *Chem. Soc. Rev.* **2010**, *39*, 1388.
(15) Sun, X.-L.; Stabler, C. L.; Cazalis, C. S.; Chaikof, E. L. *Bioconjugate Chem.* **2006**, *17*, 52.
(16) Sanchez, C.; Rozes, L.; Ribot, F.; Laberty-Robert, C.; Grosso, D.; Sassoye, C.; Boissière, C.; Nicole, L. *C. R. Chim.* **2010**, *13*, 3.
(17) Sanchez, C.; Boissière, C.; Grosso, D.; Laberty, C.; Nicole, L. *Chem. Mater.* **2008**, *20*, 682.
(18) Monton, M. R. N.; Forsberg, E. M.; Brennan, J. D. *Chem. Mater.* **2012**, *24*, 796.
(19) Derby, B. *J. Eur. Ceram. Soc.* **2011**, *31*, 2543.
(20) Lejeune, M.; Noguera, R.; Dossou-yovo, C.; Chartier, T. *J. Eur. Ceram. Soc.* **2009**, *29*, 905.
(21) Mougenot, M.; Lejeune, M.; Baumard, J. F.; Boissière, C.; Ribot, F.; Grosso, D.; Sanchez, C.; Noguera, R. *J. Am. Ceram. Soc.* **2006**, *89*, 1876.
(22) Kele, P.; Li, X.; Link, M.; Nagy, K.; Herner, A.; Lörincz, K.; Bénid, S.; Wolfbeis, O. S. *Org. Biomol. Chem.* **2009**, *7*, 3486.
(23) Arrachart, G.; Carcel, C.; Trens, P.; Moreau, J. J. E.; Wong Chi Man, M. *Chem.—Eur. J.* **2009**, *15*, 6279.
(24) Fousseret, B.; Mougenot, M.; Rossignol, F.; Baumard, J.-F.; Soulestin, B.; Boissière, C.; Ribot, F.; Jalabert, D.; Carrion, C.; Sanchez, C.; Lejeune, M. *Chem. Mater.* **2010**, *22*, 3875.
(25) Rivera-Muñoz, E. M.; Huirache-Acuña, R. *Int. J. Mol. Sci.* **2010**, *11*, 3069.
(26) Grosso, D.; Cagnol, F.; Soler-Illia, G.; Crepaldi, E.; Amenitsch, H.; Brunet-Bruneau, A.; Bourgeois, A.; Sanchez, C. *Adv. Funct. Mater.* **2004**, *14*, 309.
(27) Matheron, M.; Bourgeois, A.; Gacoin, T.; Brunet-Bruneau, A.; Albouy, P.-A.; Boilot, J.-P.; Biteau, J.; Lacan, P. *Thin Solid Films* **2006**, *495*, 175.
(28) Hesse, M.; Meier, H; Zeeh, B. *Spectroscopic Methods in Organic Chemistry*; Thieme Medical Publishers: New York, 1997.
(29) Rohlfing, D. F.; Rathousky, J.; Rohlfing, Y.; Bartels, O.; Wark, M. *Langmuir* **2005**, *21*, 11320.
(30) Beijer, F. H.; Sijbesma, R. P.; Vekemans, J. A. J. M.; Meijer, E. W.; Kooijman, H.; Spek, A. L. *J. Org. Chem.* **1996**, *61*, 6371.